



Influenza A Virus Infection Triggers Pyroptosis and Apoptosis of Respiratory Epithelial Cells through the Type I Interferon Signaling Pathway in a Mutually Exclusive Manner

SangJoon Lee,^a Mikako Hirohama,^c Masayuki Noguchi,^{a,b} Kyosuke Nagata,^c Atsushi Kawaguchi^{a,c,d}

^aPh.D. Program in Human Biology, School of Integrative and Global Majors, University of Tsukuba, Tsukuba, Japan

^bDepartment of Pathology, Faculty of Medicine, University of Tsukuba, Tsukuba, Japan

^cDepartment of Infection Biology, Faculty of Medicine, University of Tsukuba, Tsukuba, Japan

^dTransborder Medical Research Center, University of Tsukuba, Tsukuba, Japan

ABSTRACT Respiratory epithelial cell death by influenza virus infection is responsible for the induction of inflammatory responses, but the exact cell death mechanism is not understood. Here we showed that influenza virus infection induces apoptosis and pyroptosis in normal or precancerous human bronchial epithelial cells. Apoptosis was induced only in malignant tumor cells infected with influenza virus. In human precancerous respiratory epithelial cells (PL16T), the number of apoptotic cells increased at early phases of infection, but pyroptotic cells were observed at late phases of infection. These findings suggest that apoptosis is induced at early phases of infection but the cell death pathway is shifted to pyroptosis at late phases of infection. We also found that the type I interferon (IFN)-mediated JAK-STAT signaling pathway promotes the switch from apoptosis to pyroptosis by inhibiting apoptosis possibly through the induced expression of the *Bcl-xL* anti-apoptotic gene. Further, the inhibition of JAK-STAT signaling repressed pyroptosis but enhanced apoptosis in infected PL16T cells. Collectively, we propose that type I IFN signaling pathway triggers pyroptosis but not apoptosis in the respiratory epithelial cells in a mutually exclusive manner to initiate proinflammatory responses against influenza virus infection.

IMPORTANCE Respiratory epithelium functions as a sensor of infectious agents to initiate inflammatory responses along with cell death. However, the exact cell death mechanism responsible for inflammatory responses by influenza virus infection is still unclear. We showed that influenza virus infection induced apoptosis and pyroptosis in normal or precancerous human bronchial epithelial cells. Apoptosis was induced at early phases of infection, but the cell death pathway was shifted to pyroptosis at late phases of infection under the regulation of type I IFN signaling to promote proinflammatory cytokine production. Taken together, our results indicate that the type I IFN signaling pathway plays an important role to induce pyroptosis but represses apoptosis in the respiratory epithelial cells to initiate proinflammatory responses against influenza virus infection.

KEYWORDS apoptosis, pyroptosis, respiratory epithelial cells, type I IFN signaling

Respiratory epithelium is involved in physical segregation of hosts from a vast array of antigens, pollutions, and infectious agents. The respiratory epithelial cells also function as a sensor of infectious agents to initiate inflammatory responses along with cell death by infection. Various pathogens cause mainly three programmed cell death pathways: apoptosis, necroptosis, and pyroptosis (1–3). Apoptosis is a caspase-3-dependent cell death, and apoptotic cells are rapidly phagocytized and cleared without inflammatory responses (4). Necroptosis is a receptor-interacting protein 1 (RIP1) and

Received 7 March 2018 Accepted 1 May 2018

Accepted manuscript posted online 9 May 2018

Citation Lee S, Hirohama M, Noguchi M, Nagata K, Kawaguchi A. 2018. Influenza A virus infection triggers pyroptosis and apoptosis of respiratory epithelial cells through the type I interferon signaling pathway in a mutually exclusive manner. *J Virol* 92:e00396-18. <https://doi.org/10.1128/JVI.00396-18>.

Editor Adolfo García-Sastre, Icahn School of Medicine at Mount Sinai

Copyright © 2018 American Society for Microbiology. All Rights Reserved.

Address correspondence to Atsushi Kawaguchi, ats-kawaguchi@md.tsukuba.ac.jp.

RIP3 kinase complex-dependent but caspase-independent inflammatory cell death that operates by releasing damage-associated molecular patterns (DAMPs) (5). Pyroptosis is a caspase-1-dependent inflammatory cell death controlled by inflammasomes, multi-protein complexes consisting of caspase-1, apoptosis-associated speck-like protein containing a caspase recruitment domain (ASC), and cytoplasmic pathogen recognition receptors (PRRs) such as nucleotide-binding and oligomerization domain (NOD)-like receptor family proteins. The formation of inflammasomes induced by virus infection is observed mainly in immune cells and results in the extracellular release of proinflammatory cytokines, such as interleukin-1 β (IL-1 β) and IL-18 (6, 7). Influenza A virus (IAV) induces inflammatory responses as a result of respiratory epithelial cell death (8, 9). The proinflammatory response from respiratory epithelial cells triggers migration of immune cells, including macrophages and neutrophils, to remove infectious agents. These migrated immune cells contribute to excessive inflammation, which leads to pneumonia. Thus, the inflammatory response mechanism of the respiratory epithelium is crucial for understanding the pathogenesis of IAV. However, it has been reported that apoptosis is a major cell death pathway triggered by IAV infection in cultured epithelial cells isolated from malignant tumors (10–12). Therefore, the exact cell death mechanism responsible for inflammatory responses that may determine the pathogenesis of IAV is still unclear.

Emerging evidence has shown the cross talk of programmed cell death pathways (4), but the molecular mechanism to determine one of the cell death pathways remains poorly understood. Because caspase-8 activated by apoptotic stimuli suppresses necroptosis by cleaving substrates such as RIP1 and RIP3 kinases (13, 14), necroptosis is induced by the addition of caspase inhibitors in response to several stimuli. Although endogenous inhibitors of caspase-8 to induce necroptosis are not understood, virally encoded caspase inhibitors are well-known examples that promote necroptosis (5). It is well known that several proapoptotic proteins, including cytochrome *c*, are released from dysfunctional mitochondria. The dysfunctional mitochondria also activate inflammasome assembly through mitochondrial reactive oxygen species (ROS) (15), released mitochondrial DNA (16, 17), and cardiolipin (18), but the exact role of mitochondria in pyroptosis activation remains controversial (19). It is reported that mitochondrial antiviral-signaling protein (MAVS), which is an adapter molecule to transduce the type I interferon (IFN) signaling pathway triggered by a viral RNA sensor RIG-I, interacts with NOD-like receptor protein 3 (NLRP3) and stimulates inflammasome formation (20, 21). Although it is reported that RIG-I activates inflammasome through a type I IFN positive-feedback loop in respiratory epithelial cells (22), type I IFN has been shown to negatively regulate the inflammasome formation in macrophages (23). Thus, despite considerable progress in understanding each cell death pathway, it remains controversial how viruses induce each cell death, possibly due to differences in the stimuli and cell types used.

Here we showed that IAV infection induces apoptosis and pyroptosis but not necroptosis in normal or precancerous human bronchial epithelial cells. In contrast, IAV infection induced apoptosis in infected malignant tumor cells only. Apoptosis was triggered at early phases of infection, while pyroptosis was induced at late phases of infection in human precancerous respiratory epithelial (PL16T) cells. Importantly, apoptosis was inhibited by stimulation of type I IFN signaling pathway in PL16T cells, possibly through the expression of the *Bcl-xL* anti-apoptotic gene. Further, the inhibition of the JAK-STAT pathway, which is downstream of type I IFN, repressed pyroptotic cell death but enhanced apoptotic cell death in PL16T cells. Collectively, we propose that type I IFN signaling pathway triggers pyroptosis but not apoptosis in the respiratory epithelial cells in a mutually exclusive manner to initiate proinflammatory responses against IAV infection.

RESULTS AND DISCUSSION

Precancerous respiratory epithelial cells induce pyroptotic cell death in response to infection. To determine whether respiratory epithelial cell lines are susceptible to the cell death induced by IAV infection, we carried out trypan blue dye

exclusion assays at 24 h postinfection with different types of human malignant tumor respiratory epithelial cells (A549, PC9, H1975, H1650, and HCC827), human atypical adenomatous hyperplasia (AAH) respiratory epithelial cells (PL16T), human nonneoplastic respiratory epithelial cells (PL16B), and primary normal human bronchial epithelial cells (NHBE). The cell death in all malignant tumor cell lines was rarely induced by IAV infection, whereas the number of dead cells in PL16T, PL16B, and NHBE lines was 30 to 40% of total cells at 24 h postinfection (Fig. 1A). PL16T is an immortalized cell line that was established from a precancerous region of a lung adenocarcinoma patient (24). It has been reported that PL16T cells do not have any tumorigenic activity and there are no mutations or abnormal expressions of oncogenesis-related genes, such as *p53*, *Akt*, and *EGFR* (25). To determine what kinds of cell death pathways are activated by IAV infection, we treated infected PL16T, NHBE, and A549 cells with each type of cell death inhibitor: Z-DEVD-FMK (caspase-3 inhibitor) (Fig. 1B, D, F, and H), VX-765 (caspase-1 inhibitor) (Fig. 1C, E, G, and I), and GSK-872 (RIP3 inhibitor) with Z-VAD-FMK (pancaspase inhibitor) (Fig. 1J, K, and L). In infected PL16T cells, the number of dead cells either stained with trypan blue dye (Fig. 1B) or having fragmented DNA (Fig. 1D) was reduced by the addition of the caspase-3 inhibitor at 12 and 24 h postinfection, but not after 36 h postinfection. In contrast, the caspase-1 inhibitor repressed cell death even at 36 h postinfection in infected PL16T cells (Fig. 1C and E). These results suggest that apoptosis is induced in infected PL16T cells at early phases of infection but the cell death pathway is shifted to pyroptosis at late phases of infection. Similar results were obtained with infected NHBE cells (Fig. 1F and G). Furthermore, the number of dead cells in infected A549 cells was decreased by the caspase-3 inhibitor in both early and late phases of infection, but not by the caspase-1 inhibitor (Fig. 1H and I). Thus, it is likely that IAV infection triggers both apoptotic and pyroptotic cell deaths in precancerous or normal human respiratory epithelial cells but only apoptotic cell death in malignant tumor cells. GSK-872 did not inhibit cell death by IAV infection in PL16T cells, NHBE cells, and A549 cells (Fig. 1J, K, and L). These results indicate that necroptosis merely occurs in response to IAV infection in the cultured cells that we used. However, it has been reported that necroptosis is triggered by IAV infection in a mouse model (26) and immortalized murine cells, including lung epithelial cells and embryonic fibroblast cells (27). Thus, it is possible that necroptosis is stimulated by IAV infection in a species- and/or cell type-dependent manner as previously reported in other virus infections such as herpes simplex virus (28), human cytomegalovirus (29), and human immunodeficiency virus (30) infections. Note that the expression level of viral protein NP in PL16T cells was similar to that in A549 cells, indicating that the virus infectivity was comparable between A549 cells and PL16T cells (Fig. 1M).

IAV infection induces inflammasome assembly and IL-1 β secretion in human respiratory epithelial cells. To confirm whether apoptosis and pyroptosis are induced in PL16T cells by IAV infection, we examined the proteolytic activations of caspase-3 (Fig. 2A) and caspase-1 (Fig. 2B) and gasdermin D (Fig. 2C). The cell lysates prepared from infected cells at 24 h (Fig. 2A) and 48 h (Fig. 2B and C) postinfection were subjected to Western blotting analyses with anti-procaspase-3, anti-cleaved caspase-3, anti-caspase-1, and anti-gasdermin D antibodies. Camptothecin (CPT), a potent inhibitor of DNA topoisomerase-I, was used as a positive control for apoptosis induction (Fig. 2A, lane 3). Caspase-3, caspase-1, and gasdermin D were cleaved in IAV-infected PL16T cells (Fig. 2A, lane 7; Fig. 2B, lane 6; Fig. 2C, lane 2) but not when each caspase inhibitor was added (Fig. 2A, lanes 4 and 6; Fig. 2B, lanes 4 and 5; Fig. 2C, lane 3).

Upon inflammasome formation, ASC is assembled into a micrometer-sized perinuclear structure called an ASC speck to recruit procaspase-1 for its proteolytic self-activation. Then, the activated caspase-1 cleaves several substrates such as gasdermin D for pyroptosis induction and also activates the secretion of inflammatory cytokines IL-1 β and IL-18 by digestion of their immature forms (31). Inflammasomes have been extensively characterized in monocytes and macrophages but not epithelial cells, although epithelial cells may play an important role in early host immune response to infection. To examine whether inflammasomes are formed, we carried out indirect

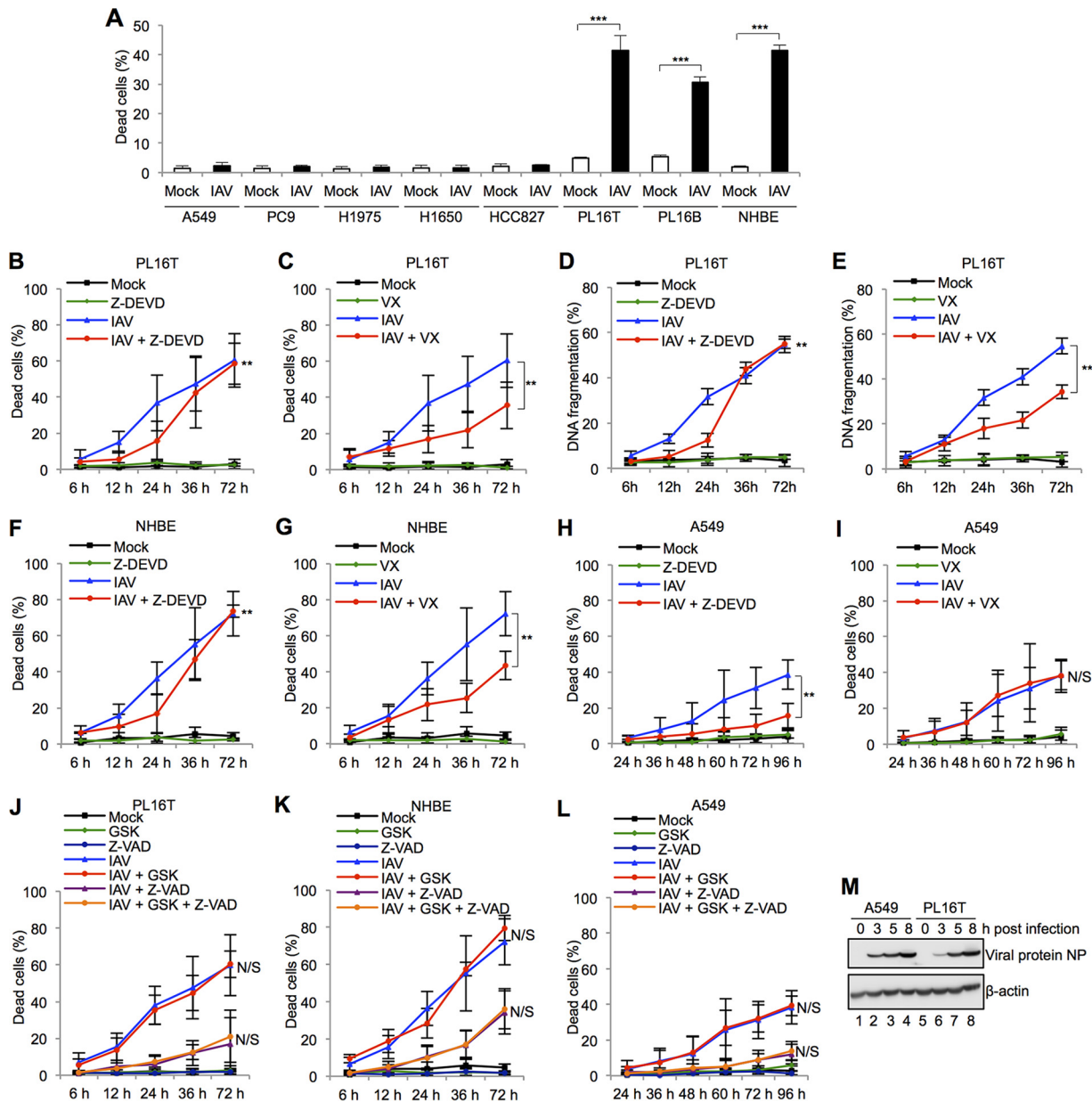


FIG 1 Influenza virus infection induces pyroptotic cell death in precancerous respiratory epithelial cells. (A) The numbers of dead cells by IAV infection in human malignant respiratory epithelial cells (A549, PC9, H1975, H1650, HCC827), human atypical adenomatous hyperplasia (AAH) respiratory epithelial cells (PL16T), human nonneoplastic respiratory epithelial cells (PL16B), and primary normal human bronchial epithelial cells (NHBE) were determined by trypan blue dye exclusion assays. The data represent averages with standard deviations from three independent experiments ($n > 100$). ***, $P < 0.001$ by Student's t test. (B to L) PL16T cells (B, C, D, E, and J), NHBE cells (F, G, and K), and A549 cells (H, I, and L) were infected with IAV at an MOI of 10 in the presence of 10 μ M Z-DEVD-FMK (Z-DEVD; caspase-3 inhibitor) (B, D, F, and H), 20 μ M VX-765 (VX; caspase-1 inhibitor) (C, E, G, and I), and 3 μ M GSK-872 (GSK; RIP3 inhibitor) with 20 μ M Z-VAD-FMK (Z-VAD; pan-caspase inhibitor) (J, K, and L). The number of dead cells was measured by trypan blue dye exclusion assays, and the cells with fragmented DNA were quantified by ArrayScan high-content systems. The data represent averages with standard deviations from three independent experiments ($n > 100$). **, $P < 0.01$ by two-way analysis of variance (ANOVA); N/S, not significant. (M) At 3, 5, and 8 h postinfection, infected A549 (lanes 1 to 4) and PL16T cells (lanes 5 to 8) were lysed, and the lysates were analyzed by SDS-PAGE followed by Western blotting assays using anti-NP and anti- β -actin antibodies.

immunofluorescence assays with anti-ASC antibody in PL16T, NHBE, and A549 cells. At 48 h postinfection, ASC specks were observed in approximately 30% of total PL16T and NHBE cells but not in A549 cells (Fig. 2D). We next examined IL-1 β secretion from PL16T, NHBE, and A549 cells in response to IAV infection by enzyme-linked immunosorbent assays (ELISA). At 72 h postinfection, approximately 50 pg/ml of IL-1 β was secreted from infected PL16T and NHBE cells; however, we could not detect IL-1 β

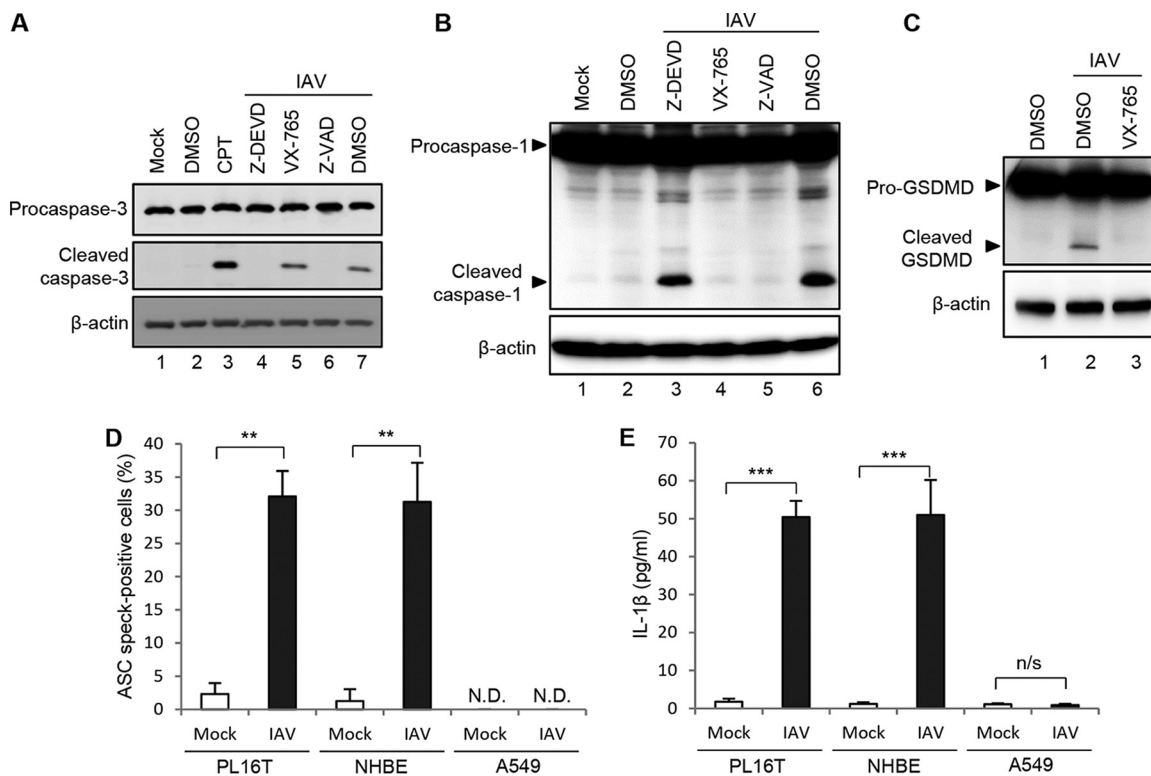


FIG 2 IAV infection induces inflammasome assembly and IL-1 β secretion in human respiratory epithelial cells. (A) Infected PL16T cells were incubated with either 10 μ M Z-DEVD-FMK, 20 μ M VX-765, or 20 μ M Z-VAD-FMK for 24 h, and then the cell lysates were subjected to Western blot analysis with anti-procaspase-3 and anti-cleaved caspase-3 antibodies. As a positive control, cells were treated with 10 μ M camptothecin (CPT) to activate caspase-3. β -Actin was detected as a loading control. DMSO, dimethyl sulfoxide. (B) Infected PL16T cells were incubated with either 10 μ M Z-DEVD-FMK, 20 μ M VX-765, or 20 μ M Z-VAD-FMK for 48 h, and then the cell lysates were subjected to Western blot analysis using anti-caspase-1 antibody. β -Actin was detected as a loading control. (C) Infected PL16T cells were incubated with 20 μ M VX-765 for 48 h, and then the cell lysates were subjected to Western blot analysis using anti-GSDMD antibody. β -Actin was detected as a loading control. (D) At 48 h postinfection, uninfected and infected PL16T, NHBE, and A549 cells were subjected to indirect immunofluorescence assays using anti-ASC antibody, and the percentages of ASC speck-positive cells were quantitated. The data represent averages with standard deviations from three independent experiments ($n > 100$). (E) PL16T, NHBE, and A549 cells were infected with IAV at an MOI of 10. At 72 h postinfection, cell-free supernatants were collected and the concentration of IL-1 β was quantified by ELISA. The data represent averages with standard deviations from three independent experiments. **, $P < 0.01$; ***, $P < 0.001$ by Student's t test; N.D., not detected; n/s, not significant.

secretion from infected A549 cells (Fig. 2E). It has been reported that along with the establishment of malignancy in tumor microenvironment, genetic mutations and epigenetic modifications are induced, leading to abnormal expression of genes related to cell death and cell survival, such as *p53* and *Akt* (32, 33). Upon carcinogenesis, tissue homeostasis is disorganized, and then this leads to inflammatory responses to recruit immune cells at the tumor microenvironment to eliminate the tumor cells (34). Thus, only immunosilent tumor variants would develop into malignant tumor cells. We found that malignant respiratory epithelial cells weakly induced only apoptosis in response to IAV infection (Fig. 2D and E). This suggests that signaling pathways to trigger pyroptosis may decline along with the tumor development, thereby allowing cells to escape from cancer immunosurveillance.

The type I IFN signaling pathway triggers pyroptosis but represses apoptosis in a mutually exclusive manner. Next, we examined the number of apoptotic and pyroptotic cells by indirect immunofluorescence assays with anti-cleaved caspase-3 and anti-ASC antibodies to distinguish each cell death pathway (Fig. 3A). About 35% of infected cells were stained with anti-cleaved caspase-3 antibody at 24 h postinfection, and the signals were reduced at 36 h postinfection along with the apoptotic cell fragmentation (Fig. 3B). In contrast, the number of ASC speck-positive cells peaked at 48 h postinfection (Fig. 3C). This is in good agreement with the results shown in Fig. 1B

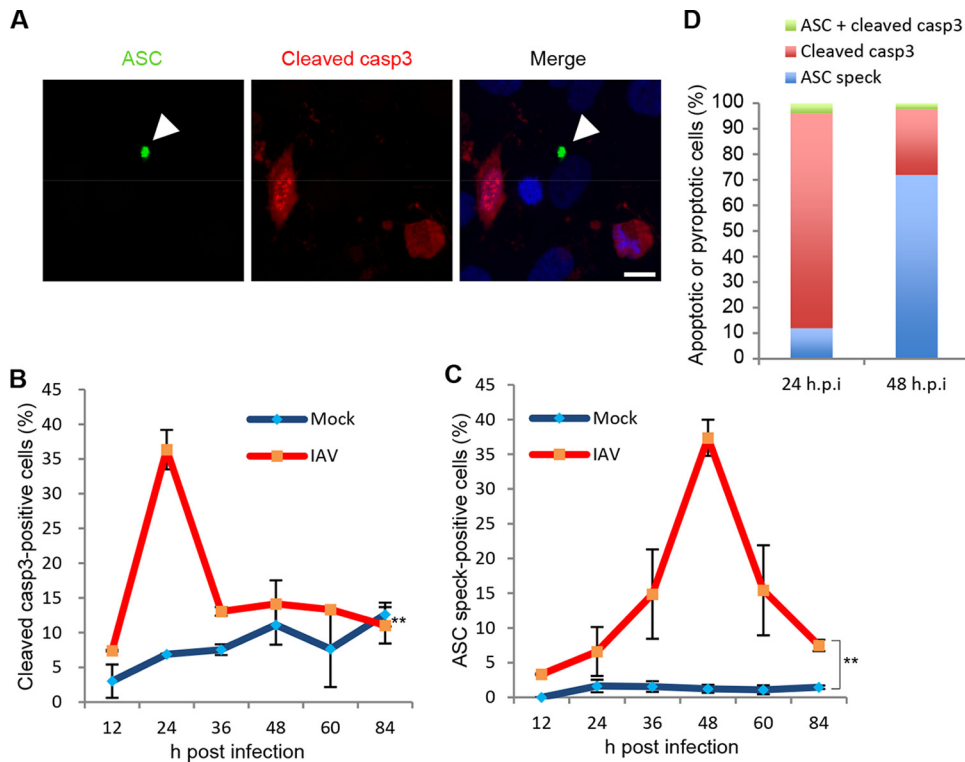


FIG 3 Apoptosis and pyroptosis are independently induced in PL16T cells against IAV infection. (A to D) At 12, 24, 36, 48, 60, and 84 h postinfection, uninfected and infected PL16T cells were subjected to indirect immunofluorescence assays with anti-ASC (green) and anti-cleaved caspase-3 (red) antibodies. A representative result at 24 h postinfection is shown in panel A. Arrowheads indicate ASC inflammasome. Bar, 10 μ m. The average numbers of cleaved caspase-3-positive (B) and ASC speck-positive (C) cells and standard deviations obtained from three independent experiments are shown ($n > 100$). The percentages of cleaved caspase-3-positive (red), ASC speck-positive (blue), and cleaved caspase-3/ASC speck-positive (green) cells were determined at 24 and 48 h postinfection (D). **, $P < 0.01$ by two-way ANOVA.

and C. Further, both cleaved caspase-3- and ASC speck-positive cells were hardly observed (Fig. 3A and D), suggesting that apoptosis and pyroptosis are independently induced by IAV infection in PL16T cells.

The viral nonstructural protein NS1 is a multifunctional RNA binding protein and is known to be an important regulator of host immune responses and apoptotic cell death. NS1 inhibits double-stranded RNA (dsRNA)-mediated protein kinase R (PKR) activation and IFN- β production through its RNA binding activity (35). NS1 also prevents IFN- β production by inhibiting the activation of RIG-I through the interaction with TRIM25 (36). NS1 activates phosphatidylinositol 3-kinase (PI3K) signaling by binding to the p85 β regulatory subunit of PI3K (37). This results in the activation of Akt kinase, and the activated Akt protein phosphorylates proapoptotic Bcl-2 family proteins to inhibit apoptosis. We next examined the number of apoptotic and pyroptotic cells triggered by the IAV NS1 mutants listed below: the R38A/K41A mutant, which is deficient in dsRNA-binding activity and in IFN antagonism (35); the Y89F mutant, which is deficient in PI3K/Akt activation for the inhibition of proapoptotic proteins (37); and the del NS1 mutant, which contains a deletion of NS1 gene (38) (Fig. 4A). We found that the R38A/K41A mutation increased the inflammasome formation, but not the cleavage of procaspase-3, more than 5 times compared to the wild type (WT) at 24 h postinfection (Fig. 4A), suggesting that enhanced type I IFN production increases pyroptotic cell death upon IAV infection. In contrast, the Y89F mutation increased apoptosis but not pyroptosis, possibly due to the inability to inhibit proapoptotic Bcl-2 family proteins, including the Bcl-2-associated death promoter (BAD) protein (Fig. 4A). We also found that del NS1 virus infection stimulated pyroptosis, but not apoptosis, as well as

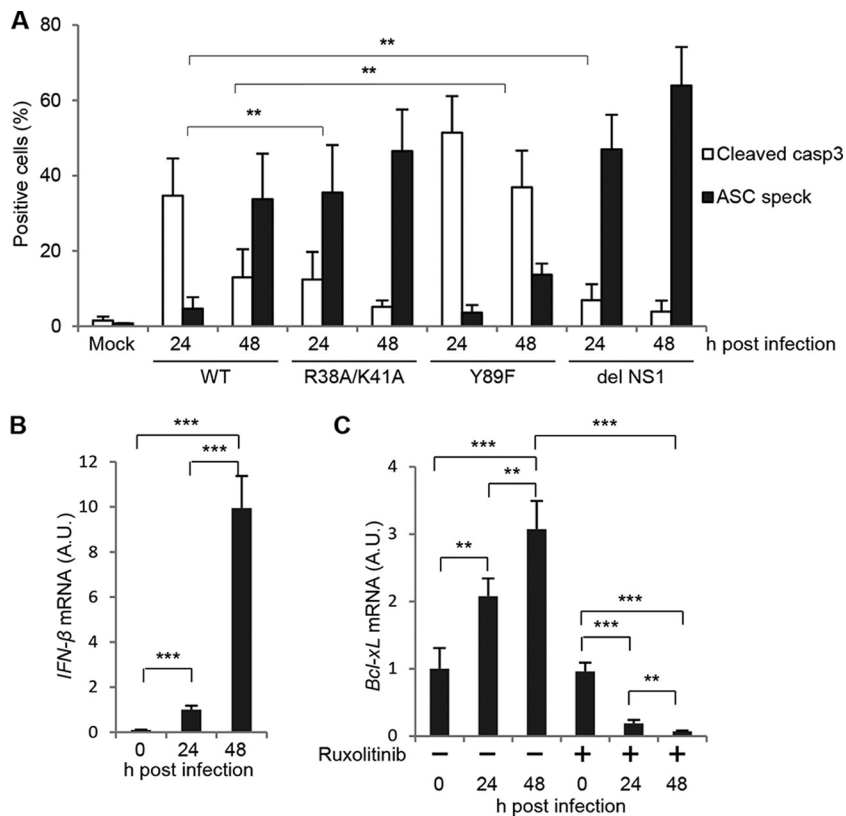


FIG 4 Apoptotic and pyroptotic cell death of respiratory epithelial cells induced by NS1 mutant viruses. (A) PL16T cells were infected with either wild-type, R38A/K41A, Y89F, or del NS1 virus. At 24 and 48 h postinfection, the cells were subjected to indirect immunofluorescence assays with anti-ASC and anti-cleaved caspase-3 antibodies. The average numbers of cleaved caspase-3-positive and ASC speck-positive cells and standard deviations obtained from three independent experiments are shown ($n > 100$). (B) PL16T cells were infected with wild-type IAV. At 24 and 48 h postinfection, cells were collected and the total RNAs were subjected to reverse transcription followed by real-time PCR with primers specific for *IFN-β* mRNA. The mean values and standard deviations obtained from three independent experiments are shown. (C) PL16T cells were infected with wild-type IAV in the absence or presence of 1 $\mu\text{g/ml}$ ruxolitinib. At 24 and 48 h postinfection, total RNAs were purified and were subjected to reverse transcription followed by real-time PCR with primers specific for *Bcl-xL* mRNA. The mean values and standard deviations obtained from three independent experiments are shown. **, $P < 0.01$; ***, $P < 0.001$ by Student's *t* test.

R38A/K41A mutant virus. This suggests that type I IFN signaling pathway may antagonize proapoptotic Bcl-2 family proteins for the mutually exclusive activation of apoptosis and pyroptosis. Note that the *IFN-β* gene was transcribed in wild-type IAV-infected PL16T cells at 48 h postinfection, although the response was not quick, possibly due to the inhibition by NS1 (Fig. 4B).

The Bcl-2 family proapoptotic BH3-only protein BAD interacts with the Bcl-xL anti-apoptotic protein to release apoptogenic factors such as cytochrome *c* from mitochondria to induce apoptosis. Akt kinase phosphorylates BAD, and the phosphorylated BAD is retained in the cytoplasm through the interaction with 14-3-3 proteins to prevent heterodimerization with Bcl-xL at the mitochondrial membrane (39, 40). It has been known that the expression level of Bcl-xL, but not Bcl-2, is regulated through STAT5, Ets, Rel/NF- κ B, and AP-1 transcription factors in response to survival signaling pathways (41), although the effect of IAV infection on Bcl-xL expression is still unclear. To address this, we examined the amount of *Bcl-xL* mRNA in infected PL16T cells in the absence or presence of 1 $\mu\text{g/ml}$ ruxolitinib, a potent inhibitor of the JAK-STAT signaling pathway that is downstream of the type I IFN receptor. The level of *Bcl-xL* mRNA was increased about three times by IAV infection in PL16T cells, and this increase was significantly repressed by ruxolitinib treatment (Fig. 4C). Therefore, it is possible that

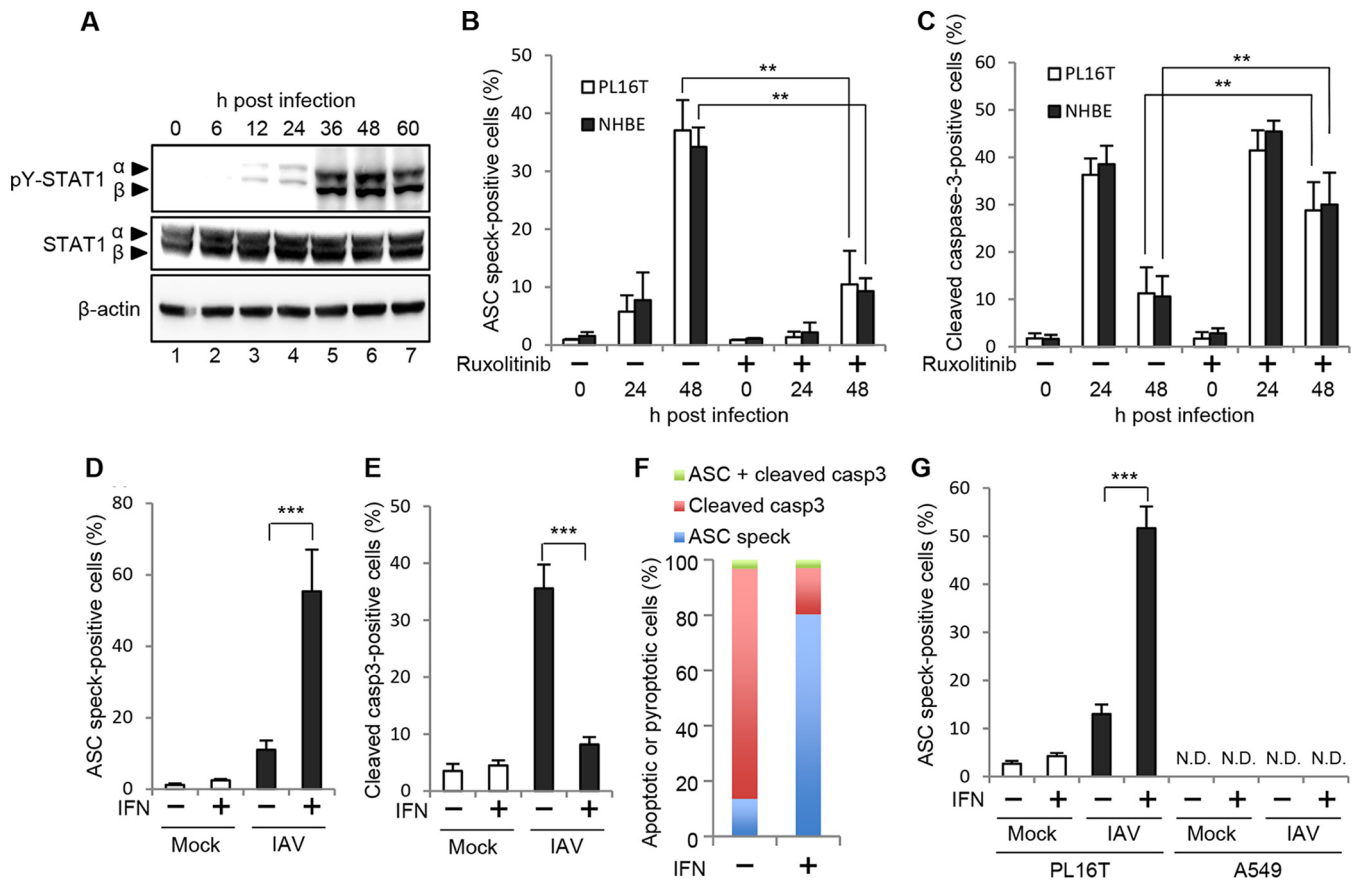


FIG 5 Type I IFN triggers pyroptosis but not apoptosis in a mutually exclusive manner. (A) At 0, 6, 12, 24, 36, 48, and 60 h postinfection, infected PL16T cells were lysed, and the cell lysates were subjected to Western blot analysis using anti-phospho-STAT1 (Tyr701) and STAT1. β -Actin was detected as a loading control. (B and C) PL16T (open bars) and NHBE (filled bars) cells were infected with IAV at an MOI of 10 in the absence or presence of 1 μ g/ml ruxolitinib. At 24 and 48 h postinfection, PL16T and NHBE cells were subjected to indirect immunofluorescence assays using anti-cleaved caspase-3 and anti-ASC antibodies. The percentage of ASC speck-positive cells (B) and that of cleaved caspase-3-positive cells (C) are shown. The mean values and standard deviations obtained from three independent experiments are shown ($n > 100$). (D to F) At 6 h postinfection, infected PL16T cells were incubated with or without 1,000 IU/ml IFN- β . At 24 h postinfection, cells were subjected to indirect immunofluorescence assays using anti-ASC and anti-cleaved caspase-3 antibodies. The average numbers of ASC speck-positive (D) and cleaved caspase-3-positive (E) cells and standard deviations obtained from three independent experiments are shown ($n > 100$). The percentages of ASC speck-positive (blue), cleaved caspase-3-positive (red), and cleaved caspase-3/ASC speck-positive (green) cells were determined (F). (G) At 6 h postinfection, infected PL16T and A549 cells were incubated with or without 1,000 IU/ml IFN- β . At 24 h postinfection, cells were subjected to indirect immunofluorescence assays using anti-ASC antibody. The average numbers of ASC speck-positive cells and standard deviations obtained from three independent experiments are shown ($n > 100$). **, $P < 0.01$; ***, $P < 0.001$ by Student's t test; N.D., not detected.

the induced expression of Bcl-xL by the JAK-STAT pathway antagonizes proapoptotic Bcl-2 family proteins to inhibit the apoptotic cell death in infected PL16T cells.

To elucidate whether type I IFN production is involved in the mutually exclusive activation of apoptosis and pyroptosis in IAV-infected PL16T cells, we next examined the phosphorylation level of STAT1. The phosphorylation level of STAT1 increased at 36 h postinfection (Fig. 5A) concomitantly with pyroptosis activation (Fig. 3C). Further, we treated infected PL16T and NHBE cells with 1 μ g/ml ruxolitinib and performed indirect immunofluorescence assays using anti-ASC and anti-cleaved caspase-3 antibodies (Fig. 5B and C). By the addition of ruxolitinib, the number of ASC speck-positive cells decreased to approximately 30% of that in the absence of ruxolitinib (Fig. 5B). In contrast, the number of cleaved caspase-3-positive cells was increased more than 3 times by ruxolitinib treatment at 48 h postinfection (Fig. 5C). Next, to examine the effect of type I IFN on the pyroptosis induction, infected cells were treated with 1,000 IU/ml IFN- β at 6 h postinfection, at which time viral proteins are fully expressed while apoptosis is not activated (Fig. 1B and M). At 24 h postinfection, we carried out the indirect immunofluorescence assays using anti-ASC and anti-cleaved caspase-3 antibodies (Fig. 5D and E). Approximately 10% of PL16T cells showed ASC specks at 24 h

postinfection in the absence of IFN- β , and the number of ASC speck-positive cells increased to more than 50% by IFN- β treatment, as expected (Fig. 5D). In contrast, the number of cleaved caspase-3-positive cells was reduced in infected PL16T cells in the presence of IFN- β (Fig. 5E). We did not detect cells with ASC specks and cleaved caspase-3 (Fig. 5F). These findings suggest that the type I IFN signaling pathway is responsible for switching the cell death pathway from apoptosis to pyroptosis in infected respiratory epithelial cells. Note that there were no detectable ASC speck-positive A549 cells even in the presence of IFN- β (Fig. 5G), suggesting that type I IFN production is not sufficient to induce pyroptosis in malignant tumor cells in response to IAV infection.

In conclusion, our studies demonstrated that apoptosis is induced at early phases of infection but the cell death pathway is shifted to pyroptosis at late phases of infection under the regulation of type I IFN signaling to promote the production of proinflammatory cytokines. The cytokines may trigger recruitment of macrophages and neutrophils to eliminate infectious agents, including apoptotic and pyroptotic cells. Although a fraction of infected cells could escape from apoptosis, possibly by anti-apoptotic viral protein NS1, it is possible that type I IFN inhibits the virus spread through pyroptotic cell death to eliminate infected cells at late phases of infection. Further, the epithelial surfaces of respiratory tissues are exposed to the external environment, including commensal microorganisms. It is possible that type I IFN signaling may guarantee the inflammatory response specific for pathogenic infectious agents. Future studies on the physiological relevance of type I IFN-induced pyroptosis in respiratory epithelium *in vivo* are required.

MATERIALS AND METHODS

Biological materials. Influenza virus strain A/Puerto Rico/8/34 and a rabbit polyclonal antibody against NP were prepared as previously described (42). R38A/K41A and Y89F mutant viruses (A/Puerto Rico/8/34 genetic backbone) were constructed as previously described (37, 43). del NS1 virus was a generous gift from Adolfo Garcia-Sastre (Icahn School of Medicine at Mount Sinai, New York, NY). Mouse monoclonal antibodies against β -actin (A5441; Sigma), ASC (04-147; Millipore), caspase-1 (MAB6215; R&D systems), and GSDMDC1 (sc-81868; Santa Cruz Biotechnology) and rabbit polyclonal antibodies against cleaved caspase-3 (9661; Cell Signaling Technology), procaspase-3 (9662; Cell Signaling Technology), STAT1 α/β (sc-346; Santa Cruz Biotechnology), and phospho-(Tyr701) STAT1 (Cell Signaling Technology) were purchased. Z-DEVD-FMK (R&D systems), VX-765 (Chemietek), GSK-872 (Millipore), Z-VAD-FMK (Enzo Life Science), camptothecin (Calbiochem), IFN- β (Toray), and ruxolitinib (Cayman) were purchased. A549 cells were grown in Dulbecco's modified Eagle medium (DMEM) containing 10% fetal bovine serum. PC9, H1650, and HCC827 cells were grown in RPMI 1640 with 10% fetal bovine serum. H1975 cells were grown in RPMI 1640 containing high glucose with 10% fetal bovine serum. PL16T and PL16B cells were grown in MCDB153HAA medium with 0.5 ng/ml epidermal growth factor, 5 μ g/ml insulin, 72 ng/ml hydrocortisone, 10 μ g/ml transferrin, 20 ng/ml sodium selenite, and 2% fetal bovine serum (24). NHBE cells were purchased, and the cells were grown in B-ALI growth medium (Lonza).

Trypan blue dye exclusion assay. After pretreatment of cells with each cell death inhibitor for 1 h, the cells were infected with influenza virus at a multiplicity of infection (MOI) of 10. At the indicated time points, both adherent and floating cells were collected and resuspended in 0.02% trypan blue (Sigma) in phosphate-buffered saline (PBS). The dead and living cells were counted using a hemocytometer.

DNA fragmentation assay. PL16T cells (5×10^3 cells) were seeded in a 96-well optical bottom plate (Thermo) and were infected with influenza virus at an MOI of 10. At the indicated time points, the cells were stained with Hoechst 33342, and then the cells with fragmented DNA were quantified by ArrayScan high-content systems (Thermo).

Indirect immunofluorescence assays. Both adherent and floating cells were collected and fixed with 3% paraformaldehyde (PFA) for 10 min, and then the cells were permeabilized with 0.5% Triton X-100 in PBS containing 0.2% bovine serum albumin (BSA) for 3 min. After incubation in PBS containing 1% skim milk for 1 h, the cells were incubated with primary antibodies for 1 h. After washing with PBS containing 0.1% Tween 20 and 0.2% BSA, the cells were incubated with either Alexa Fluor 488- or Alexa Fluor 568-conjugated secondary antibodies, respectively (Invitrogen) for 30 min. After washing with PBS containing 0.1% Tween 20 and 0.2% BSA, the cells were transferred onto a coverslip by cytocentrifugation at $760 \times g$ for 5 min at 4°C. Images were acquired by confocal laser scanning microscopy (LSM700; Carl Zeiss) using a 63 \times Apochromat objective.

ELISA. PL16T, NHBE, and A549 cells in a 35-mm dish were infected with IAV at an MOI of 10. At 72 h postinfection, the culture supernatants were collected and the cell-free supernatants were subjected to ELISA with a human IL-1 β kit according to the manufacturer's instructions (MBL).

Quantitative real-time PCR. Total RNA was isolated from PL16T cells by the acid guanidinium phenol chloroform method. cDNA was prepared from purified RNA (1 μ g) by using ReverTraAce (Toyobo) with oligo(dT)₂₀ primer. Real-time PCR was carried out using SYBR green real-time PCR master mix-Plus

(Roche) in the thermal cycler Dice real-time PCR system (TaKaRa). Primer sequences used in this study were as follows: 5'-GCCACTTACCTGAATGACCAC-3' and 5'-TGCTGCATTGTTCCCATAGA-3' for *Bcl-xL*; 5'-TGCCTCAAGGACAGGATGAAC-3' and 5'-GCGTCTCCTTCTGGAAGT-3' for *IFN-β*; 5'-AACGGCTACCACATCCAAGG-3' and 5'-GGGAGTGGGTAATTGCGC-3' for 18S rRNA. The results were normalized to the level of 18S rRNA.

ACKNOWLEDGMENTS

We thank T. Ichinohe (The University of Tokyo) for helpful discussions. We also thank C. K. Ho (University of Tsukuba) for critical reviews of the manuscript.

This research was supported in part by a grant-in-aid from the Ministry of Education, Culture, Sports, Science, and Technology of Japan (16H05192 to A.K., 24115002 to K.N.) and the NOMURA Microbial Community Control Project of ERATO of the Japan Science and Technology Agency (A.K.).

We declare that we have no conflict of interest.

S.L. and A.K. conceived and designed the experiments; S.L. and M.H. performed the experiments; S.L., M.N., K.N., and A.K. analyzed the data; S.L., A.K., K.N., and M.N. contributed reagents/materials/analysis tools; S.L., A.K., and K.N. wrote the manuscript.

REFERENCES

- Fink SL, Cookson BT. 2005. Apoptosis, pyroptosis, and necrosis: mechanistic description of dead and dying eukaryotic cells. *Infect Immun* 73:1907–1916. <https://doi.org/10.1128/IAI.73.4.1907-1916.2005>.
- Ashida H, Mimuro H, Ogawa M, Kobayashi T, Sanada T, Kim M, Sasakawa C. 2011. Cell death and infection: a double-edged sword for host and pathogen survival. *J Cell Biol* 195:931–942. <https://doi.org/10.1083/jcb.201108081>.
- Lamkanfi M, Dixit VM. 2010. Manipulation of host cell death pathways during microbial infections. *Cell Host Microbe* 8:44–54. <https://doi.org/10.1016/j.chom.2010.06.007>.
- Creagh EM. 2014. Caspase crosstalk: integration of apoptotic and innate immune signalling pathways. *Trends Immunol* 35:631–640. <https://doi.org/10.1016/j.it.2014.10.004>.
- Cho YS, Challa S, Moquin D, Genga R, Ray TD, Guildford M, Chan FK. 2009. Phosphorylation-driven assembly of the RIP1-RIP3 complex regulates programmed necrosis and virus-induced inflammation. *Cell* 137:1112–1123. <https://doi.org/10.1016/j.cell.2009.05.037>.
- Pirhonen J, Sarenava T, Kurimoto M, Julkunen I, Matikainen S. 1999. Virus infection activates IL-1 beta and IL-18 production in human macrophages by a caspase-1-dependent pathway. *J Immunol* 162:7322–7329.
- Kanneganti TD, Body-Malapel M, Amer A, Park JH, Whitfield J, Franchi L, Taraporewala ZF, Miller D, Patton JT, Inohara N, Nunez G. 2006. Critical role for Cryopyrin/Nalp3 in activation of caspase-1 in response to viral infection and double-stranded RNA. *J Biol Chem* 281:36560–36568. <https://doi.org/10.1074/jbc.M607594200>.
- Chan MC, Cheung CY, Chui WH, Tsao SW, Nicholls JM, Chan YO, Chan RW, Long HT, Poon LL, Guan Y, Peiris JS. 2005. Proinflammatory cytokine responses induced by influenza A (H5N1) viruses in primary human alveolar and bronchial epithelial cells. *Respir Res* 6:135. <https://doi.org/10.1186/1465-9921-6-135>.
- Sanders CJ, Doherty PC, Thomas PG. 2011. Respiratory epithelial cells in innate immunity to influenza virus infection. *Cell Tissue Res* 343:13–21. <https://doi.org/10.1007/s00441-010-1043-z>.
- Wurzer WJ, Planz O, Ehrhardt C, Giner M, Silberzahn T, Pleschka S, Ludwig S. 2003. Caspase 3 activation is essential for efficient influenza virus propagation. *EMBO J* 22:2717–2728. <https://doi.org/10.1093/emboj/cdg279>.
- Daidoji T, Koma T, Du A, Yang CS, Ueda M, Ikuta K, Nakaya T. 2008. H5N1 avian influenza virus induces apoptotic cell death in mammalian airway epithelial cells. *J Virol* 82:11294–11307. <https://doi.org/10.1128/JVI.01192-08>.
- Takizawa T, Matsukawa S, Higuchi Y, Nakamura S, Nakanishi Y, Fukuda R. 1993. Induction of programmed cell death (apoptosis) by influenza virus infection in tissue culture cells. *J Gen Virol* 74(Part 11):2347–2355. <https://doi.org/10.1099/0022-1317-74-11-2347>.
- Feng S, Yang Y, Mei Y, Ma L, Zhu DE, Hoti N, Castanares M, Wu M. 2007. Cleavage of RIP3 inactivates its caspase-independent apoptosis pathway by removal of kinase domain. *Cell Signal* 19:2056–2067. <https://doi.org/10.1016/j.cellsig.2007.05.016>.
- Rebe C, Cathelin S, Launay S, Filomenko R, Prevotat L, L'Ollivier C, Gyan E, Micheau O, Grant S, Dubart-Kupperschmitt A, Fontenay M, Solary E. 2007. Caspase-8 prevents sustained activation of NF-kappaB in monocytes undergoing macrophagic differentiation. *Blood* 109:1442–1450. <https://doi.org/10.1182/blood-2006-03-011585>.
- Zhou R, Yazdi AS, Menu P, Tschopp J. 2011. A role for mitochondria in NLRP3 inflammasome activation. *Nature* 469:221–225. <https://doi.org/10.1038/nature09663>.
- Shimada K, Crother TR, Karlin J, Dagvadorj J, Chiba N, Chen S, Ramanujan VK, Wolf AJ, Vergnes L, Ojcius DM, Rentsendorj A, Vargas M, Guerrero C, Wang Y, Fitzgerald KA, Underhill DM, Town T, Arditi M. 2012. Oxidized mitochondrial DNA activates the NLRP3 inflammasome during apoptosis. *Immunity* 36:401–414. <https://doi.org/10.1016/j.immuni.2012.01.009>.
- Nakahira K, Haspel JA, Rathinam VA, Lee SJ, Dolinay T, Lam HC, Englert JA, Rabinovitch M, Cernadas M, Kim HP, Fitzgerald KA, Ryter SW, Choi AM. 2011. Autophagy proteins regulate innate immune responses by inhibiting the release of mitochondrial DNA mediated by the NALP3 inflammasome. *Nat Immunol* 12:222–230. <https://doi.org/10.1038/ni.1980>.
- Iyer SS, He Q, Janczy JR, Elliott EI, Zhong Z, Olivier AK, Sadler JJ, Knepper-Adrian V, Han R, Qiao L, Eisenbarth SC, Nauseef WM, Cassel SL, Sutterwala FS. 2013. Mitochondrial cardiolipin is required for Nlrp3 inflammasome activation. *Immunity* 39:311–323. <https://doi.org/10.1016/j.immuni.2013.08.001>.
- Allam R, Lawlor KE, Yu EC, Mildenhall AL, Moujalled DM, Lewis RS, Ke F, Mason KD, White MJ, Stacey KJ, Strasser A, O'Reilly LA, Alexander W, Kile BT, Vaux DL, Vince JE. 2014. Mitochondrial apoptosis is dispensable for NLRP3 inflammasome activation but non-apoptotic caspase-8 is required for inflammasome priming. *EMBO Rep* 15:982–990. <https://doi.org/10.15252/embr.201438463>.
- Subramanian N, Natarajan K, Clatworthy MR, Wang Z, Germain RN. 2013. The adaptor MAVS promotes NLRP3 mitochondrial localization and inflammasome activation. *Cell* 153:348–361. <https://doi.org/10.1016/j.cell.2013.02.054>.
- Chakrabarti A, Banerjee S, Franchi L, Loo YM, Gale M, Jr, Nunez G, Silverman RH. 2015. RNase L activates the NLRP3 inflammasome during viral infections. *Cell Host Microbe* 17:466–477. <https://doi.org/10.1016/j.chom.2015.02.010>.
- Pothlichet J, Meunier I, Davis BK, Ting JP, Skamene E, von Messling V, Vidal SM. 2013. Type I IFN triggers RIG-I/TLR3/NLRP3-dependent inflammasome activation in influenza A virus infected cells. *PLoS Pathog* 9:e1003256. <https://doi.org/10.1371/journal.ppat.1003256>.
- Guarda G, Braun M, Staehli F, Tardivel A, Mattmann C, Forster I, Farlik M, Decker T, Du Pasquier RA, Romero P, Tschopp J. 2011. Type I interferon inhibits interleukin-1 production and inflammasome activation. *Immunity* 34:213–223. <https://doi.org/10.1016/j.immuni.2011.02.006>.
- Shimada A, Kano J, Ishiyama T, Okubo C, Iijima T, Morishita Y, Minami Y, Inadome Y, Shu Y, Sugita S, Takeuchi T, Nouguchi M. 2005. Establishment of an immortalized cell line from a precancerous lesion of lung adenocarcinoma.

- carcinoma, and genes highly expressed in the early stages of lung adenocarcinoma development. *Cancer Sci* 96:668–675. <https://doi.org/10.1111/j.1349-7006.2005.00100.x>.
25. Noguchi M. 2010. Stepwise progression of pulmonary adenocarcinoma—clinical and molecular implications. *Cancer Metastasis Rev* 29: 15–21. <https://doi.org/10.1007/s10555-010-9210-y>.
 26. Rodrigue-Gervais IG, Labbe K, Dagenais M, Dupaul-Chicoine J, Champagne C, Morizot A, Skeldon A, Brincks EL, Vidal SM, Griffith TS, Saleh M. 2014. Cellular inhibitor of apoptosis protein cIAP2 protects against pulmonary tissue necrosis during influenza virus infection to promote host survival. *Cell Host Microbe* 15:23–35. <https://doi.org/10.1016/j.chom.2013.12.003>.
 27. Nogusa S, Thapa RJ, Dillon CP, Liedmann S, Oguin TH, III, Ingram JP, Rodriguez DA, Kosoff R, Sharma S, Sturm O, Verbist K, Gough PJ, Bertin J, Hartmann BM, Sealfon SC, Kaiser WJ, Mocarski ES, Lopez CB, Thomas PG, Oberst A, Green DR, Balachandran S. 2016. RIPK3 activates parallel pathways of MLKL-driven necroptosis and FADD-mediated apoptosis to protect against influenza A virus. *Cell Host Microbe* 20:13–24. <https://doi.org/10.1016/j.chom.2016.05.011>.
 28. Guo H, Omoto S, Harris PA, Finger JN, Bertin J, Gough PJ, Kaiser WJ, Mocarski ES. 2015. Herpes simplex virus suppresses necroptosis in human cells. *Cell Host Microbe* 17:243–251. <https://doi.org/10.1016/j.chom.2015.01.003>.
 29. Omoto S, Guo H, Talekar GR, Roback L, Kaiser WJ, Mocarski ES. 2015. Suppression of RIP3-dependent necroptosis by human cytomegalovirus. *J Biol Chem* 290:11635–11648. <https://doi.org/10.1074/jbc.M115.646042>.
 30. Gaiha GD, McKim KJ, Woods M, Pertel T, Rohrbach J, Barteneva N, Chin CR, Liu D, Soghoian DZ, Cesa K, Wilton S, Waring MT, Chicoine A, Doering T, Wherry EJ, Kaufmann DE, Lichterfeld M, Brass AL, Walker BD. 2014. Dysfunctional HIV-specific CD8⁺ T cell proliferation is associated with increased caspase-8 activity and mediated by necroptosis. *Immunity* 41:1001–1012. <https://doi.org/10.1016/j.immuni.2014.12.011>.
 31. Liu X, Zhang Z, Ruan J, Pan Y, Magupalli VG, Wu H, Lieberman J. 2016. Inflammasome-activated gasdermin D causes pyroptosis by forming membrane pores. *Nature* 535:153–158. <https://doi.org/10.1038/nature18629>.
 32. Guo G, Marrero L, Rodriguez P, Del Valle L, Ochoa A, Cui Y. 2013. Trp53 inactivation in the tumor microenvironment promotes tumor progression by expanding the immunosuppressive lymphoid-like stromal network. *Cancer Res* 73:1668–1675. <https://doi.org/10.1158/0008-5472.CAN-12-3810>.
 33. Crane CA, Panner A, Murray JC, Wilson SP, Xu H, Chen L, Simko JP, Waldman FM, Pieper RO, Parsa AT. 2009. PI(3) kinase is associated with a mechanism of immunoresistance in breast and prostate cancer. *Oncogene* 28:306–312. <https://doi.org/10.1038/onc.2008.384>.
 34. Coussens LM, Werb Z. 2002. Inflammation and cancer. *Nature* 420: 860–867. <https://doi.org/10.1038/nature01322>.
 35. Donelan NR, Basler CF, Garcia-Sastre A. 2003. A recombinant influenza A virus expressing an RNA-binding-defective NS1 protein induces high levels of beta interferon and is attenuated in mice. *J Virol* 77: 13257–13266. <https://doi.org/10.1128/JVI.77.24.13257-13266.2003>.
 36. Gack MU, Albrecht RA, Urano T, Inn KS, Huang IC, Carnero E, Farzan M, Inoue S, Jung JU, Garcia-Sastre A. 2009. Influenza A virus NS1 targets the ubiquitin ligase TRIM25 to evade recognition by the host viral RNA sensor RIG-I. *Cell Host Microbe* 5:439–449. <https://doi.org/10.1016/j.chom.2009.04.006>.
 37. Hale BG, Jackson D, Chen YH, Lamb RA, Randall RE. 2006. Influenza A virus NS1 protein binds p85beta and activates phosphatidylinositol-3-kinase signaling. *Proc Natl Acad Sci U S A* 103:14194–14199. <https://doi.org/10.1073/pnas.0606109103>.
 38. Garcia-Sastre A, Egorov A, Matassov D, Brandt S, Levy DE, Durbin JE, Palese P, Muster T. 1998. Influenza A virus lacking the NS1 gene replicates in interferon-deficient systems. *Virology* 252:324–330. <https://doi.org/10.1006/viro.1998.9508>.
 39. Zha J, Harada H, Yang E, Jockel J, Korsmeyer SJ. 1996. Serine phosphorylation of death agonist BAD in response to survival factor results in binding to 14-3-3 not BCL-X(L). *Cell* 87:619–628. [https://doi.org/10.1016/S0092-8674\(00\)81382-3](https://doi.org/10.1016/S0092-8674(00)81382-3).
 40. Datta SR, Dudek H, Tao X, Masters S, Fu H, Gotoh Y, Greenberg ME. 1997. Akt phosphorylation of BAD couples survival signals to the cell-intrinsic death machinery. *Cell* 91:231–241. [https://doi.org/10.1016/S0092-8674\(00\)80405-5](https://doi.org/10.1016/S0092-8674(00)80405-5).
 41. Sevilla L, Zaldumbide A, Pognonec P, Boulukos KE. 2001. Transcriptional regulation of the bcl-x gene encoding the anti-apoptotic Bcl-xL protein by Ets, Rel/NFkappaB, STAT and AP1 transcription factor families. *Histol Histopathol* 16:595–601.
 42. Kawaguchi A, Hirohama M, Harada Y, Osari S, Nagata K. 2015. Influenza virus induces cholesterol-enriched endocytic recycling compartments for budzone formation via cell cycle-independent centrosome maturation. *PLoS Pathog* 11:e1005284. <https://doi.org/10.1371/journal.ppat.1005284>.
 43. Moriyama M, Chen IY, Kawaguchi A, Koshiba T, Nagata K, Takeyama H, Hasegawa H, Ichinohe T. 2016. The RNA- and TRIM25-binding domains of influenza virus NS1 protein are essential for suppression of NLRP3 inflammasome-mediated interleukin-1beta secretion. *J Virol* 90: 4105–4114. <https://doi.org/10.1128/JVI.00120-16>.